Creep behavior inb a fine-grained Al -5356 alloy at low stress and intermediate temperature

Shen, Junjie
Department of Molecular and Materials Science, Graduate student

Ikeda, Ken-ichi
Department of Electrical and Material Science, Kyushu University

Hata, Satoshi
Department of Electrical and Material Science, Kyushu University

Nakashima, Hideharu
Department of Electrical and Material Science, Kyushu University

https://doi.org/10.15017/19574

出版情報：九州大学大学院総合理工学報告. 33 (1), pp.1-6, 2011-06. 九州大学大学院総合理工学府
バージョン：
権利関係：

九州大学大学院総合理工学府報告
第33巻 第1号 1-6 頁 平成23年6月

Engineering Sciences Reports, Kyushu University
Vol. 33, No. 1, pp. 1-6, JUN, 2011

Creep behavior in a fine-grained Al-5356 alloy at low stress and intermediate temperature

Junjie SHEN [*1,†] Ken-ichi IKEDA[*2] Satoshi HATA [*2]
and Hideharu NAKASHIMA[*2]
[†]E-mail of corresponding author: *nk-j-shen@mms.kyushu-u.ac.jp*

(Received April 27, 2011)

Creep in an Al-5356 solid solution alloy with an intercept grain size, $d_g = 5 \pm 0.5$ μm was investigated using the helicoid spring specimen technique. The testing temperatures ranged from 423 K to 523 K (0.47 to 0.58 T_m) and the applied stresses from 0.20 MPa to 4.02 MPa. It was found that under the above conditions, viscous creep of Bingham type occurs, characterized by a threshold stress which decreases with increasing temperature. The activation energy is Q_c = 44 ± 7 kJ/mol. No microstructural changes were observed in recrystallized and the as-crept specimens. The measured creep rates were found to be four orders faster than that predicted by Coble creep model.

Key words: *Helicoid spring specimen technique, Intermediate temperature, Low-stress creep*

1. Introduction

The creep deformation of materials at low stress and intermediate temperature, $0.4\,T_m < T < 0.6\,T_m$ (T_m: melting temperature) often exhibits the characters: the stress exponent is $n = 1$, and the activation energy, Q_c, is close to grain boundary diffusional energy[1-6] or dislocation core diffusion energy[7-11]. The corresponding viscous creep mechanisms and creep testing techniques are listed in Table 1. Those creep mechanisms are dependent on grain sizes. Harper-Dorn type creep controlled by dislocation core diffusion motion[7,8] occurs at a large intercept grain size (d_g > 120 μm), while for a small intercept grain size (d_g < 120 μm) coble type creep controlled by diffusional transport of matters via grain boundaries[1] or Singarn-Nix type creep by shearing along slip band accommodated by diffusion flow[12] is activated. However, "H-D creep at intermediate temperature" is still ambiguous[14], and lacks the support of dislocation substructures. As for coble creep, there are the discrepancies between theory and experimental data[15].

In addition, the creep behavior and mechanism at intermediate in precipitate-strengthened fine-grained materials are still unclear, partly because the creep in those materials at intermediate temperature and low stress will yield to very low strain rate, $\dot{\varepsilon} < 10^{-10}\ s^{-1}$. In this range, direct measurement of steady-state creep rates by the traditional uniaxial creep technique is difficult due to very small magnitudes of strain, and very long duration of creep tests. As another experimental technique, the helicoid spring technique has been employed, because the helicoid spring creep test provides the highest strain sensitivity in contrast to conventional compression and tension tests [16]. A helicoid spring sample was used in the creep test for the first time by Eakin[17] and this technique was then elaborated by Burton and others[18-22]. Intensive works on low-strain rate creep using helicoid spring specimens have been done by Fiala and Čadek[23, 24]. More recently, lots of studies on the low-strain rate creep behavior of various materials (heat-resistant steal, Ni-15%Cr solid solution alloy and pure aluminum) have been reported by Kloc et al. [2, 3, 25-27]. Those results provided creep data that are important to analyze creep mechanisms at ultra-low, $\dot{\varepsilon}$, and it was revealed that extrapolation from power-law creep regime to low stress conditions can cause serious underestimation of predicted deformation rates. However, most notably, and in contrast to compression and tension testing, in spring testing the stress and strain are not uniform through the specimen's cross section. The stress and strain generally increase from the center to the surface, where the values are at a maximum. Because of that, stress redistribu-

*1 Department of Molecular and Materials Science, Graduate student
*2 Department of Electrical and Material Science

tion will occur under the condition that creep behavior is non-viscous. It is possible to find the correct solution from a series of tests at various load levels by solving the appropriate integral equations numerically described by Kloc et al.. [28)]

The purpose of this study is to investigate the creep behavior and mechanism in precipitate-strengthened Al-5356 Mg solute-solution alloy with an intercept grain size, $d_g = 5 \pm 0.5$ μm, at low stress and intermediate temperature ranging from 423 K to 523 K (0.47 ~ 0.58 T_m) using the helicoid spring specimen technique.

Table 1 Basic mechanisms of creep at low stress and intermediate temperature.

Creep model	Deformation process	Rate-controlling process	Accommodating process	Microstructural characters	Creep rate dependence on d, or λ	Reference		
						Theory	Experiment	Testing technique
Coble	Diffusional transport of matter via grain boundaries	Grain boundary diffusion	Grain boundary sliding		$1/d^3$	[1]	[2-6]	Unaxial [4-6] Multiaxial (helicoid spring creep) [2,3]
Harper-Dorn	Motion of lattice dislocations	Dislocation core diffusion		Jogged screw dislocations	none	[7,8]	[7-11]	Multiaxial (helicoid spring creep) [7-11]
Singar n-Nix	Shearing along slip band	The climb of dislocations at grain boundaries	Grain boundary diffusion	Slip bands	d/λ^4	[12]	[13]	Biaxial (hoop creep) [13]

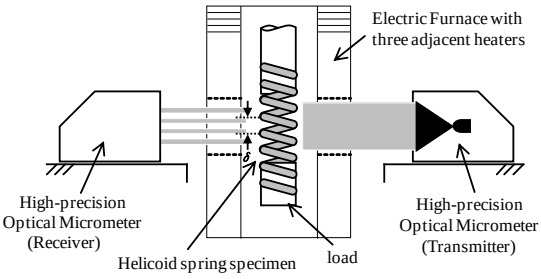

Fig. 1 The scheme of the helicoid-spring creep machine.

2 Experimental

The experiments were performed on Al-5356 Mg solid-solution alloy in the form of wires with a diameter, d = 1.6 mm. Its Chemical composition by weight percent is as follows: 4.81 Mg, 0.13 Fe, 0.08 Si, 0.01 Cu, 0.07 Mn, 0.08 Cr, and the balance is Al. Helicoid spring specimens with a mean coil diameter, D = 18.8 mm, were prepared by winding the wires on threaded stainless steel bolts. The bolts with the wound wires were heat-treated in air at 723 K for 48 h to fix the helicoid shape and obtain fully recrystallized microstructure. The intercept grain size is 5 ± 0.5 μm.

Creep tests were performed at temperature, T= 423 K, 473 K and 523 K, and applied stress, $\sigma \leq 10$ MPa, using the helicoid spring technique. Figure 1 illustrates the apparatuse of helicoid spring creep tests which has three adjacent heaters that are independently controlled to obtain uniform temperature distribution in the helicoid sample with an accuracy of ± 1 K during creep deformation. The pitches of the helicoids of the sample were measured using a light-emitting diode with an accuracy of 0.5 μm.

The following equations[29, 30)] have been employed to calculate the mean surface shear stress, τ, and the surface shear strain, γ, assuming pure torsion of the helicoid spring specimen:

$$\tau = \frac{8PD}{\pi d^3}, \quad (1)$$

$$\gamma = \frac{\delta d}{\pi D^2}, \quad (2)$$

where P is the average load, D is the coil diameters, d is the wire diameters and δ is the average rate of deflection. Since the stress and strain in the helicoids spring are essentially shear ones, they are transformed to the equivalent tensile quantities using the a well known relations, tension stress $\sigma = \sqrt{3}\tau$ and tensile strain $\varepsilon = \gamma/\sqrt{3}$. In the present study at low stress, the initial coil pitch spacing is δ = 2.5 mm. During creep tests, δ change from 2.5 mm to 3.5 mm. Our earlier investigation[31)] on the relation between torsion and normal elastic strains in Sn-Ag helicoid spring analyzed by the finite element method revealed that one can neglect the normal elastic strains under the condition of the coil pitch spacing between 0 to 5 mm. Therefore, the creep deformation in the present study can be considered as to be only torsion strains. Though, the normal elastic strain cannot be neglect at high stress, in this study the creep behavior at high stress has been also investigated by this technique to give a direct evidence on the creep mechanism change.

Microstructures in recrystallized and as-crept specimens were observed by transmission electron microscopy (TEM). TEM observation area is middle parts of cross sections of the wires. Thin foils for the TEM observation were prepared by mechanical polishing and twin-jet electropolishing using a mixture of 30% HNO_3 and 70% methanol at 243 K. The TEM observation was conducted with a JEOL JEM-2000EX/T transmission electron microscope operated at 200 kV of the accelerating voltage.

3. Results

3.1 Stress dependence of steady state creep rate

An example of creep curves obtained at 423 K and different stresses is shown in Fig. 2. The creep curves clearly show that transient creep rate decreasing with the testing time increasing. After a relatively short period of transient creep, steady state creep commences.

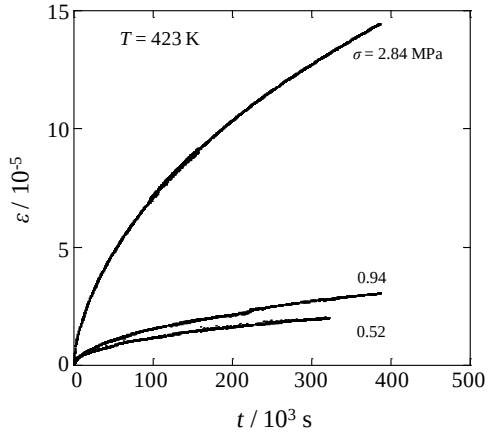

Fig. 2 Typical creep curves obtained by helicoid spring creep technique at test temperature, 423 K.

The applied stress, σ, less than 3 MPa dependence of steady-state creep rate, $\dot{\varepsilon}_s$, in linear relations is shown in Fig. 3. It is apparent that the steady-state creep rate is characterized by a Bingham viscous behavior, and hence it is proportional to the difference between the applied stress and a threshold stress, τ_o. In this case, redistribution of the stress across the coil wire cross-section occurs during creep. This problem was analysed by Crossland *et al.*[32] who showed that the stress redistribution is manifested by a slight transient creep component and that in the steady state it influences only the value of threshold stress ($\tau_{ov} = 3/4\,\tau_o$ where τ_{ov} is the threshold stress corrected for the stress redistribution and τ_o is that of measured values) as obtained by extrapolation of the creep rate-stress relation to zero creep rate.

The threshold stresses are ranging from 0.08 to 0.21 MPa for experimental data and 0.06 to 0.16 MPa for corrected data, and is taken into account in principle. Temperature dependence of the threshold stress is shown in Fig. 4. It can be described as:

$$\sigma_0 = A - B\frac{T}{T_m} \qquad (3)$$

where A = 0.771 and B = 0.901 (melting temperature, T_m = 901 K). The figure shows that the threshold stress decreases with increas of temperature.

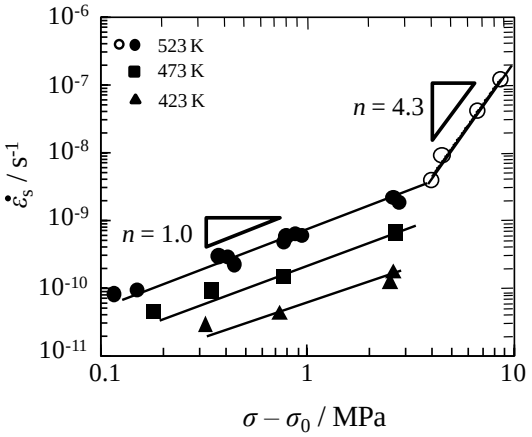

Fig. 3 Relation between steady-state creep rate and applied stress in double linear coordinates at T = 423, 473 and 523 K.

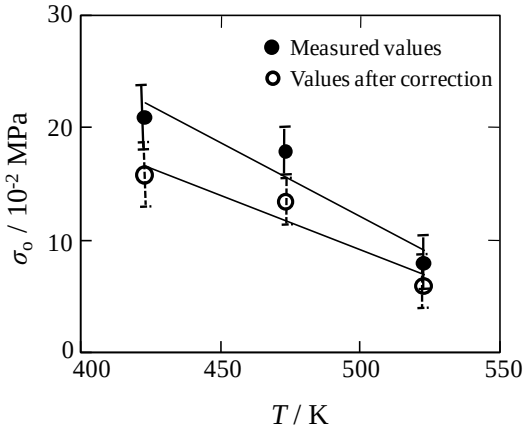

Fig. 4 Temperature dependence on threshold stress, σ_0. , experimental data; , corrected for the stress redistribution .

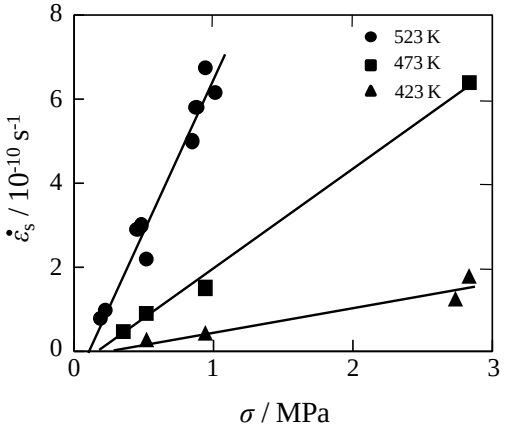

Fig. 5－Stress, $\sigma - \sigma_0$, dependence of steady-state creep rate in double logarithm coordinates at T = 423, 473 and 523 K respectively.

A plot of stress, $\sigma - \sigma_0$, against the steady-state creep rate, $\dot{\varepsilon}_s$, in double logarithm obtained by the helicoid spring creep tests for different temperatures is shown in Fig. 5. It is apparent that creep mechanism has changed. In low stress creep region, a stress exponent is equal to 1, whereas the value is 4.3 at high stress.

3.2 Temperature dependence of steady-state creep rate

The activation energy, Q_c, values were determined by fitting the data to the Arrhenius equation:

$$\dot{\varepsilon}_s = A\exp\left(-\frac{Q_c}{RT}\right) \quad (4)$$

where A is a constant depended on materials and stress, R is the universal gas constant, T is the testing temperature. Fig. 6 shows $\dot{\varepsilon}_s$ in logarithmic scale plotted against the reciprocal temperature, $1/T$ for low stress creep region (n = 1). The activation energy values of 44 ± 7 kJ / mol was obtained. The value is around 0.26-0.36 Q_L (Q_L is lattice diffusion energy of Al, and 142 kJ / mol[33]), and slightly less than that for grain boundary diffusion (0.33 Q_L < Q_{gb} < 0.67 Q_L).

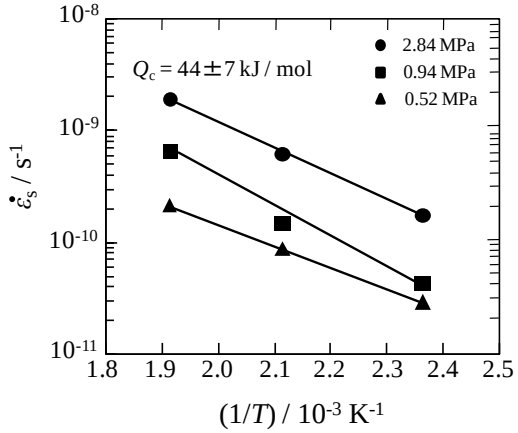

Fig. 6 Temperature dependence on the steady-state creep rate.

3.3 Microstructural observation

TEM was used to study the fine structural details in the recrystallized and as-crept specimens at low stress. Fig. 7 (a) shows a representative bright-field TEM micrography of the recrystallized specimens. That clearly depicts the equiaxed grain structure present in the annealed materials and precipitates located in the grain and grain boundary. No evidence for the existence of dislocations is revealed by tilting the specimen. A representative bright-field TEM micrography in the specimen crept to a steady-state creep stage at T = 423 K and σ = 0.42 MPa is shown in Fig. 7 (b). One cannot find the existence of dislocations by tilting this specimen, and apparent change of microstructures. It should be noted that there is a possibility that grain growth may occur during creep, which generally leads to a change in the stress exponents. However, the microstructural studies following creep do not indicate that the occurrence of any such grain growth. In addition, if grain growth did occur during creep, the rates of growth at different test conditions will be different, and it is not expected that the strain-rate data will follow the linear stress variation as observed in this study.

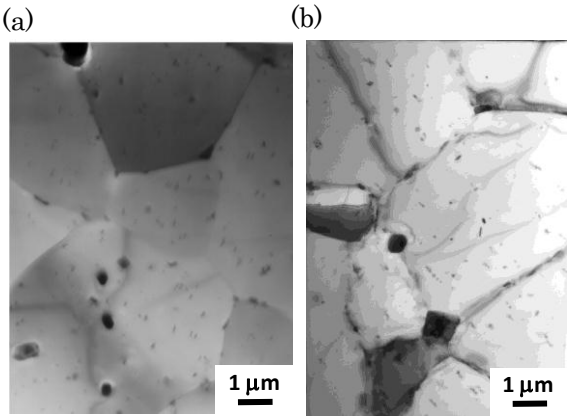

Fig. 7 TEM micrographs. (a) In the annealed materials. (b) In the specimen crept to the steady-state stage at 423 K and 0.42 MPa.

3. Discussion

The stress exponent is n = 1. One of possible mechanisms is that creep controlled by Coble creep. To clearly establish Coble creep as the rate-controlling mechanism, the steady-state creep rates obtained at 523 K are compared to the standard Coble creep model predications. The Coble creep model is described by the following equation[34]:

$$\frac{\dot{\varepsilon}kT}{D_{gb}Eb} = 22.4\left(\frac{b}{d}\right)^3\left(\frac{\sigma}{E}\right)^1 \quad (5)$$

where D_{gd} is the diffusion coefficient along a grain boundary ($D_{gd} = D_0\exp[-Q_{gb}/RT]$, where D_0 is a frequency factor, Q_{gb} is a grain boundary diffusion, b is the magnitude of Burgers vector, k is Boltzmann's constant, 1.38

$\times 10^{-23}$ J·K^{-1}, T is the absolute temperature, σ is the applied stress and d is an average intercept grain size. In this study, the following values are set: d_g = 5 μm, D_0 = 1.70 × 10^{-4} m^{2}s^{-1} [35], Q_{gb}= 85.2 kJ/mol = 0.6 Q_L [35], and b = 2.86×10^{-10} m. A good agreement between the actual strain rates and the Coble creep model predications would indicate Coble creep as the rate-controlling mechanism. Alternatively, calculating the model prefactor and comparing it with standard standard prefactor for Coble creep would serve as a good verification. It was observed that Coble constant for the data points corresponding to 523 K are 1×10^4 that is higher than the theoretical Coble constant value, i.e. 22.4 shown in Fig. 8. In that case, it is predicted that creep behavior cannot be described by Coble creep.

Slip band mechanism and "Harper-Dorn creep controlled by dislocation core diffusion at intermediate temperature" can also be excluded because the microstructural observation did not show the formation of slip band[14] as expected in slip band mechanism and jogged screw dislocations as expected in "Harper-Dorn creep at intermediate temperature[7, 8]". In addition, Harper-Dorn creep is generally expected to occur in a relatively larger grain.

The experimental results: stress exponent equal to 1, creep activation energy ranging from 0.26 Q_L to 0.37 Q_L and no change of microstructure in recrystallized and as-crept specimens, can not be explained with available creep theories.

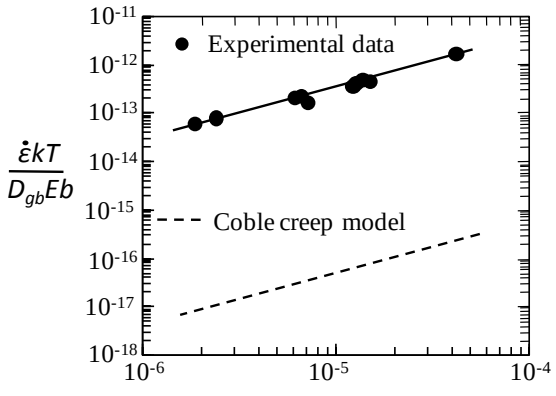

Fig. 8 Correlation of this study with theoretical Coble creep model at 423 K.

4. Summary

Creep tests were carried out on an Al-5356 Mg solid-solution alloy with intercept grain size, $d_g = 5 \pm 0.5$ μm in the form of wires by helicoid spring creep technique at intermediate temperature (0.47 to 0.58 T_m) and low stress (0.20 to 4.02 MPa). The viscous creep of Bingham type occurs, characterized by a threshold stress which decreases with increasing temperature. The activation energy was $Q_c = 44 \pm 7$ kJ / mol that is slightly less than that for grain boundary diffusion (0.33 Q_L < Q_{gb} < 0.67 Q_L). The measured creep rates were about four orders faster than expected Coble creep. No microstructural changes were observed in the recrystallized and as-crept specimens. The creep behavior cannot be explained by the creep models: Coble creep, "Harper-Dorn creep at intermediate temperature" and Slip-band creep mechanism.

Acknowledgments

This work was supported in part by Grants-in-Aid from the Japan Society for the Promotion of Science (JSPS) and Grants-in-Aid from the Ministry of Education, Culture, Science and Technology (MEXT), Japan.

References

1) R.L. Coble, J. Appl. Phys., 34 (1963) 1679.
2) L. Kloc, J. Fiala and J. Čadek, Mater. Sci. Eng. A, 130 (1990) 165.
3) L. Kloc, J. Fiala and J. Čadek, Mater. Sci. Eng. A, 202 (1995) 11.
4) W.J. Kim, Scripta Mater., 58 (2008) 659.
5) R.B. Jones, Nature, 207 (1965) 70.
6) I. Charit and A.H. Chokshi, Acta Metall., 49 (2001) 2239.
7) J. Novotný, J. Fiala and J. Čadek, Acta Metall., 33 (1985) 905.
8) J. Novotný, J. Fiala and J. Čadek, Scripta Mater., 19 (1985) 867.
9) J. Fiala, J. Novotný and J. Čadek, J. Mater. Sci. Eng., 1983, vol. 60, pp. 195.
10) G. Malakondaiah and P. Rama Rao, Acta Metall., 1981, vol. 29, pp. 1263.
11) G. Malakondaiah and P. Rama Rao, Mater. Sci. Eng., 52 (1982) 207.
12) H. Fukuyo, H.C. Tsai, T. Oyama and O.D. Sherby, ISIJ Int., vol. 31, (1991) pp. 76.
13) S. Gollapudi, I. Charit and K.L. Murty, Acta Metall., vol. 56, (2008) pp. 2406.
14) L. Kloc and J. Fiala, Mater. Sci. Eng. A, 410 (2005) 38.
15) O. A. Ruano and O. D. Sherby, Mater. Sci. Eng., 1982, vol. 56, pp. 167.
16) L. Kloc and P. Mareček, Journal of Testing and Evaluation, 2009, vol. 37, pp. 53.
17) C.T. Eakin: Prod. Eng. (N.Y.), 1956, vol. 27, pp. 186.
18) B. Burton and G.W. Greenwood, Met. Sci. J, 4 (1970) 215.
19) B. Burton and G.L. Reynold, Acta Metall., 21 (1973) 1073.
20) I.G. Crossland, R.B. Jones and G.W. Lewthwaite, J. Physic D, 6 (1973) 1040.
21) D.J. Towle and H. Jones, Acta Metall., 24 (1976) 399.
22) B. Burton, Acta Metall., 26 (1978) 1237.

23) A. Ball and M.M. Hutchison, J. Metall. Sci., 3 (1969) 1.
24) J. Novotný, J. Fiala and J. Čadek, Acta Metall., 3 (1985) 905.
25) L. Kloc and V. Skleni*č*ka, Mater. Sci. Eng. A, 234 (1997), 962.
26) L. Kloc, V. Skleni*č*ka and J. Ventruba, Mater. Sci. Eng. A, 319 (2001) 774.
27) L. Kloc and V. Skleni*č*ka, Mater. Sci. Eng. A, 387 (2004) 633.
28) L. Kloc, J. Fiala and J. Čadek, Mater. Sci. Eng. A, 202 (1990) 61.
29) S. Timoshenko and D.H. Yong, Elements of Strength of Materials, fifth ed., Van Nostrand, New York, 1968, pp. 77.
30) A.M. Wahi, Mechanical Springs, second edition, McGraw-Hill, New York, 1963, pp. 229.
31) M. Ishibashi, K. Fujimoto, K. Ikeda, S. Hata and H. J. Nakashima, Japan Inst. Metals, 73 (2009) 373.
32) I. G. Crossland, R. B. Jones and G. W. Levthewaite, J. PHYS. D, 6 (1973) 1040.
33) T. S. Lundy and J. F. Murdock: J. Appl. Phys., 1962, vol. 33, pp. 1671.
34) K. Kitazono: Jpn. Inst. Light Metals, 59 (2009), 458.
35) H. Luthy, A. K. Miller and O. D. Sherby, Acta Metall., 28 (1980) 169.
36) T. Mori, S. Onaka and K. Wakashima: J. Appl. Phys., 1998, vol. 83, pp. 12-17.
37) F. W. Grossman and M. F. Ashby: Acta Metall., 1975, vol. 23, pp. 425-440.